

Numerical modeling of intra-band tunneling for heterojunction solar cells in SCAPS

J. Verschraegen*, M. Burgelman¹

University of Gent, Electronics and Information Systems (ELIS), Pietersnieuwstraat 41, B-9000 Gent, Belgium

Available online 29 January 2007

Abstract

For heterojunction solar cells with a spike in one of the bands at the junction, intra-band tunneling will enhance the current through the interface. We have incorporated this phenomenon in SCAPS, a publicly available one-dimensional solar cell device simulator. The thermionic-field emission boundary conditions at the interfaces are formulated based on the WKB approximation and we discuss the changes to the equations used in our model. We have taken care to make our model self consistent and point out differences with previous attempts to incorporate intra-band tunneling in a numerical device simulator.

We show new simulations on our model of the Cu–In–S on Cu-tape (CISCuT) solar cell. At the interface between the CuI buffer layer and the CuInS₂ absorber a spike is present in the valence band. We perform simulations with and without the inclusion of intra-band tunneling and conclude that the effect of the spike on the current transport properties of the CuI/CuInS₂ interface poses no limitations on cell efficiency.

© 2006 Elsevier B.V. All rights reserved.

Keywords: Modelling; Tunneling; CISCuT

1. Introduction

For the moment, not many numerical solar cell device simulators are capable of handling tunneling mechanisms, such as band-to-band tunneling, tunneling enhanced recombination or intra-band tunneling [1]. However, measurements have shown that these mechanisms can dominate the solar cell characteristics. As a first step in our ongoing attempt to handle all kinds of tunneling phenomena, we have included a model in SCAPS, which describes intra-band tunneling at a heterointerface. SCAPS is a one-dimensional solar cell device simulator, developed at ELIS, University of Gent, which is freely available to the PV research community [2]. The user can define a solar cell as a series of layers with different properties, such as: thickness, doping densities and defect distribution. It is then possible to simulate a number of common measurements: $I-V$, QE , $C-f$, $C-V$.

In the second section we will get into the details of the theoretical model that we used to describe intra-band tunneling. In the third section we will perform simulations on a model of the

CISCuT solar cell, including intra-band tunneling. The CISCuT solar cell (Cu–In–S₂ on Cu-Tape) is a flexible solar cell based on CuInS₂ [3]. Efficiencies over 9% on small areas and over 7% on small modules have been reported [4]. Best results have been obtained on cells with a CuI buffer layer. The resulting stack of layers can be seen in Fig. 1. A close-up of the band diagram in the vicinity of the CuI/CuInS₂ interface region is also shown. The influence of the height of the spike in the valence band on solar cell performance will be investigated with the new version of SCAPS.

2. Theoretical model

Tunneling of electrons through a potential barrier is a quantum-mechanical phenomenon. To describe it correctly one should write down the Schrödinger equation for electrons with energy below the barrier tip. This gives a differential equation which can be solved in principal and would result in electron wave vectors, from which the tunnel probability can be calculated. However, the numerical solution is not straightforward and requires great computational power. As is the habit in such a case, we will therefore use the WKB approximation for the tunneling probability [5]. A good discussion on the limitations of the WKB approximation can be found in [6].

In SCAPS a solar cell structure is defined as a number of semiconductor layers, each with its own properties. Before

* Corresponding author. Tel.: +32 9 264 3381; fax: +32 9 264 3594.

E-mail addresses: Johan.Verschraegen@elis.ugent.be (J. Verschraegen), Marc.Burgelman@elis.ugent.be (M. Burgelman).

¹ Tel.: +32 9 264 3381; fax: +32 9 264 3594.

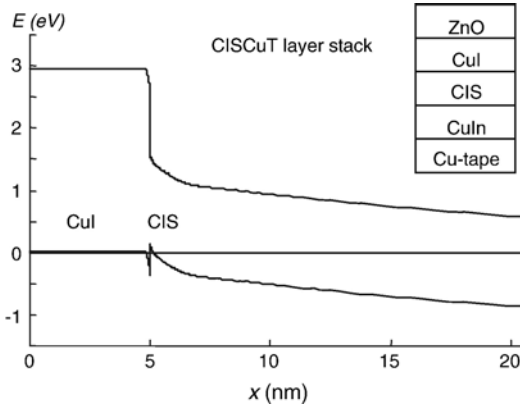


Fig. 1. Part of the energy band diagram of the CISCuT solar cell with CuI buffer layer near the CuI/CIS interface. Note the large spike in the valence band. In the upper right corner the layer sequence of the complete CISCuT device is schematically shown.

solving the equations governing the physics of the cell, a one-dimensional mesh is created and each layer is subdivided in a number of nodes or grid points. In Fig. 2 the conduction band minimum and electron quasi-Fermi level at an interface between two materials with a different electron affinity is drawn. Each dot represents a node of the one-dimensional mesh. Notice that at the interface two nodes have the same position x , but one lies in the layer to the left of the junction and the other in the layer to the right. Without the inclusion of tunneling in our models, the current at the interface is calculated as a thermionic emission current. A difference in quasi-Fermi energy at both sides of the interface is the driving force, giving the following expression for electrons [7]:

$$J_n^{T-E} = A^* T^2 \left[\exp\left(-\frac{E_C^{\max} - E_{Fn}^{\text{left}}}{kT}\right) - \exp\left(-\frac{E_C^{\max} - E_{Fn}^{\text{right}}}{kT}\right) \right]. \quad (1)$$

A^* is the Richardson constant for which the smaller value of effective mass between the two semiconductors is used [7]. To keep the notation simple, we will eliminate the index n , denoting that the formulas are for electrons.

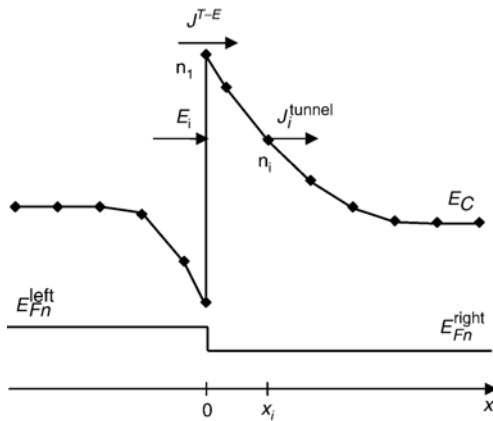


Fig. 2. Close-up of a spike in the conduction band. The dots represent the nodes of the numerical mesh. The Fermi levels E_{Fn}^{left} and E_{Fn}^{right} are also shown. The position where the thermionic emission current $J_{T-E}(x=0)$ and the tunnel current J_{tunnel} for one electron energy $E_i(x=x_i)$ are injected are marked with arrows.

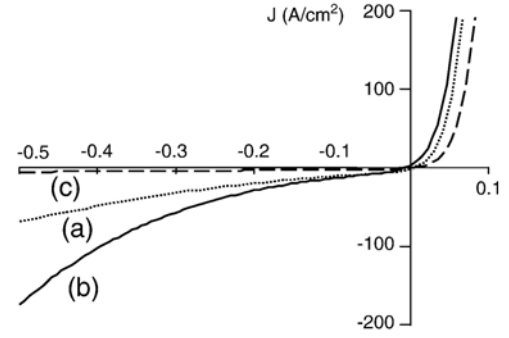


Fig. 3. Calculated J - V characteristics of an n -GaAs/ n^+ -AlGaAs test structure. (a) Yang's model [8]; all the tunnel current is injected at the interface. (b) This work; the tunnel current at energy level E is injected at the position where the level E crosses the conduction band. (c) No tunneling included.

When tunneling is considered, not only electrons at the top of the barrier, but also electrons with energy lower than E_C^{\max} can cross the interface. E_C^{\max} is the highest value of the conduction band minimum at the interface (in Fig. 1 E_C^{\max} is equal to $E_C(0^+)$). In an article by Yang et al. [8] the expression for the net electron current density crossing the interface is calculated:

$$J = -\frac{A^* T}{k} \int_{E_C^{\min}}^{\infty} f(E_x - E_{Fn}^{\text{left}}) T(E_x) dE_x + \frac{A^* T}{k} \int_{E_C^{\min}}^{\infty} f(E_x - E_{Fn}^{\text{right}}) T(E_x) dE_x \quad (2)$$

$f(E_x - E_{Fn})$ is the occupation probability (the Boltzmann distribution is used, so results for energies close to the quasi-Fermi level are not reliable). $T(E_x)$ gives the tunneling probability as derived from the WKB approximation for free electron mass [9]. It is equal to unity for energies above E_C^{\max} . The lower limit E_C^{\min} is the minimum energy level for which free electron states exist at both sides of the spike. It is the maximum of $E_C(0^-)$ and the value of E_C in the bulk of the rightmost material at the interface (in the case of Fig. 2 it would be the latter). The resulting net current is J^{T-F} , called the

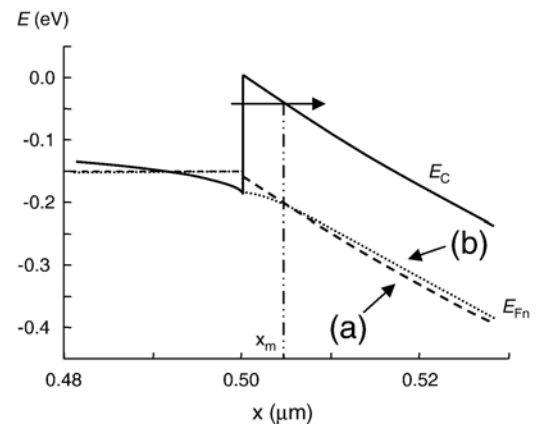


Fig. 4. Calculated energy band diagram of an n -GaAs/ n^+ -AlGaAs structure for a temperature of 150 K and under 0.5 V reverse bias. The electron quasi-Fermi level is shown for (a) Yang [8] (dashed line) and (b) this work (dotted line). The position at which the largest tunnel current is injected ($x=x_m$) is marked.

Table 1
Some of the parameters used for the GaAs/AlGaAs test structure

Property	Unit	GaAs	AlGaAs
Band gap	eV	1.42	1.73
Electron affinity	eV	4.07	3.88
Thickness	nm	500	500
Type		n	n^+
Doping density	cm^{-3}	10^{15}	5×10^{16}

thermionic-field emission current:

$$J_n^{T-F} = J_n^{T-E} (1 + \delta) \quad (3)$$

with δ equal to:

$$\delta = \frac{1}{kT} \exp\left(\frac{E_C^{\max}}{kT}\right) \int_{E_C^{\min}}^{E_C^{\max}} \exp\left(\frac{-E_x}{kT}\right) T(E_x) dE_x. \quad (4)$$

In the limit of no tunneling ($T(E_x)=0$), δ is zero, and the resulting current is equal to the thermionic emission current.

In [8] the net tunnel current is artificially injected at the interface (in Fig. 2 at $x=0$ in the node labeled n_1), together with the thermionic current. Simulations done with the use of this model are labeled (a) in Figs. 3 and 4. In SCAPS the tunnel current is injected at the turning points of the potential barrier (in Fig. 2 at $x=x_i$ at the node labeled n_i) and the position is therefore different for each electron energy (this case is labeled (b) in Figs. 3 and 4). This means that we have to keep track of the tunnel current in each grid point i (position x_i , energy $E_i=E_C(x_i)$), which we write as:

$$J_i^{\text{tunnel}} = J^{T-E} \delta_i \quad (5)$$

with

$$\delta_i = \exp\left(\frac{E_C^{\max}}{kT}\right) \exp\left(\frac{-E_i}{kT}\right) T(E_i) \frac{\Delta E_i}{kT}. \quad (6)$$

$\Delta E_i = E_C(x_i) - E_C(x_{i+1})$ is the energy interval of the conduction band between two adjacent grid points. To get the total net

Table 2
Some of the parameters used for the SCAPS model

Property	Unit	CuI	CIS 1	CIS 2	CIS 3
Band gap	eV	3.0	1.45	1.45	1.45
Electron affinity	eV	3.9	4.9	4.9	4.9
Thickness	nm	50	20	270	600
Type		p	n	n	n
Doping density	cm^{-3}	10^{20}	9×10^{17}	8×10^{15}	5.8×10^{16}

tunnel current we have to sum J_i^{tunnel} over all grid points i of the potential barrier.

In Fig. 3 a $J-V$ simulation on an n -GaAs/ n^+ -AlGaAs test structure, similar to the test structure used in [8], is presented. The most important parameters of this structure can be found in Table 1. In such a structure the hole current will be negligible and so the total current will be equal to the electron current. The temperature for which the simulation was done is 150 K. The lower the temperature, the more important the tunnel current will be compared to the thermionic emission current. Curve (a) is a simulation in which all the current is injected at the interface (node labeled n_1 in Fig. 2), while for curve (b) the tunnel current is added at the correct position (node labeled n_i in Fig. 2). It can be seen that there is a rather large difference. The energy band diagram in the neighbourhood of the interface for a reverse bias voltage of -0.5 V is shown in Fig. 4. We have arbitrarily chosen E_C^{\max} as the origin of the energy axis. The energy level of the peak tunnel current is marked with an arrow, so at the corresponding position ($x=x_m$) the most electrons are injected. The difference in quasi-Fermi energy level is clearly visible and explains the difference in $J-V$ characteristic. It should be noted that when the net tunnel current is not injected at the interface, but distributed over the barrier region, the total electron current cannot be calculated anymore as

$$J_n = \mu_n n \nabla E_{Fn} \quad (7)$$

(which only represents the drift and diffusion term of the current). We have plotted this current in Fig. 5 (a). The total current in the cell should be constant in space, and so what is missing is the tunnel current. The tunnel current per unit of

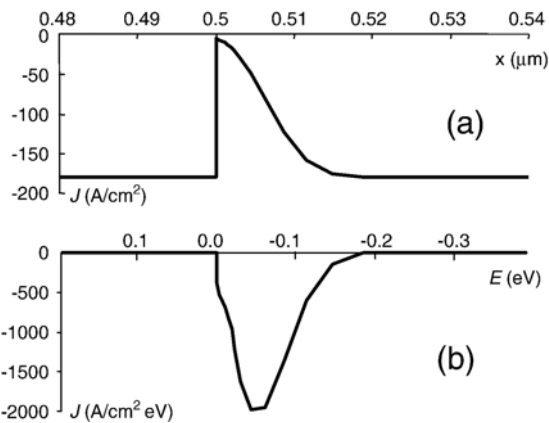


Fig. 5. (a) Calculated drift and diffusion current as a function of x , for the electron current in the n -GaAs/ n^+ -AlGaAs test structure of Fig. 4 ($T=150$ K, bias $=-0.5$ V). (b) Calculated net tunnel current per unit of energy as a function of electron energy ($E=0$, corresponds with E_C^{\max}). The integral of this current (over energies from the bottom to the top of the energy barrier) should be added to the current of (a) to get the total electron current (which is constant in space).

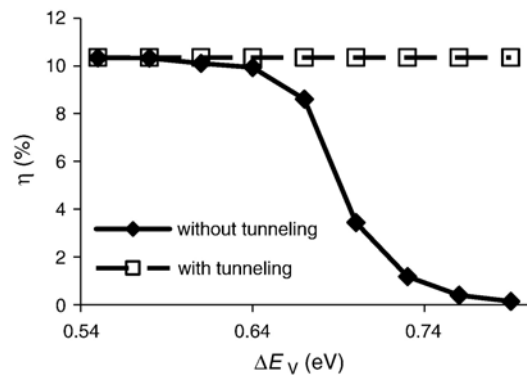


Fig. 6. Calculated influence of the valence band spike ΔE_V on the efficiency of a CISCuT solar cell, with and without intra-band tunneling present.

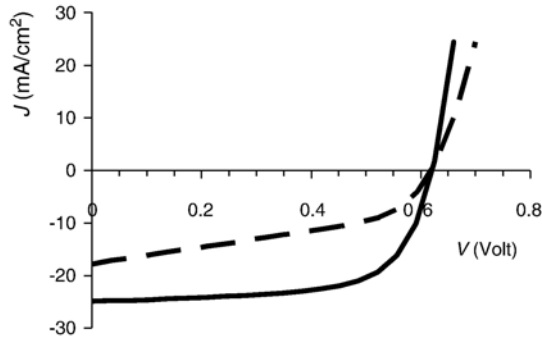


Fig. 7. Calculated J - V characteristics of a CISCuT solar cell with a valence band spike $\Delta E_V=0.69$ eV, with (solid line) and without (dashed line) intra-band tunneling included.

energy ($J_i^{\text{tunnel}}/\Delta E_i$, see Eqs. (5) and (6)) is plotted in Fig. 5 (b) as a function of energy. Again $E=0$ corresponds with E_C^{max} . Note that in Fig. 5 (a) the abscissa gives the position x in the cell, while in Fig. 5 (b) the abscissa gives the energy of the tunneling electrons E . Positions x on the top axis correspond with energies E on the bottom axis (for $x > 500$ nm) according to the relation: $E=E_C(x)$. This is an almost linear relation in the neighbourhood of the interface at a reverse bias voltage of 0.5 V (see Fig. 4). The total tunnel current at each position can be found by integrating this current over energies from the bottom to the top of the energy barrier.

3. Results

In the CISCuT solar cell (Fig. 1) at the p^+ -type CuI/ n -type CIS interface a spike is present in the valence band maximum. We will investigate with the use of SCAPS [2] whether or not this spike will limit the current through the cell and thus have a negative effect on efficiency. Due to the Anderson rule (which only holds true in the absence of an interface dipole), the height of the spike in the valence band is equal to:

$$A = E_g^{\text{CuI}} + \chi^{\text{CuI}} - E_g^{\text{CIS}} - \chi^{\text{CIS}}. \quad (8)$$

In Table 2 we show some of the parameters we used for simulations of CISCuT cells with and without the CuI buffer layer, previously reported in [10]. At that time intra-band tunneling was not yet implemented in SCAPS. How we arrive at a model with three CuInS₂ layers with different properties can be found in [10]. For the present discussion the exact structure is not important, since we are only interested in the current transport properties of the interface. The two important parameters are the spike height and the spike width, which will be determined by the CuI doping concentration. With the use of the parameters from Table 2 we arrive at a spike height of 550 meV. These parameters are however not very well known. Especially the uncertainty on the electron affinities is quite large. Therefore we have varied the spike height in our simulations by varying the value for the electron affinity of CuI (the same results are obtained when varying the electron affinity of the CuInS₂), to see what the result on cell efficiency will be.

In Fig. 6 we show simulated cell efficiency of the CISCuT structure in Fig. 1 for which we varied χ^{CuI} between 3.9 and 4.14 eV, corresponding with a spike height of 550 to 790 meV. For the curve that represents simulations for which no intra-band tunneling was incorporated, the cell efficiency drops dramatically for spike heights above 640 meV. In Fig. 7 simulated J - V curves for a spike height of 690 meV are shown for the case with and without intra-band tunneling. It is clear that the drop in efficiency is caused by a drop in short circuit current and a worsened fill factor. It is as if the potential barrier at the interface acts as a large series resistance.

When intra-band tunneling is taken into account, as it should be when one wants to do realistic simulations on the CISCuT solar cell, the spike height does not influence the J - V simulations (the cell efficiency is constant as a function of spike height, see Fig. 6). This is due to a very small spike width of about 3 nm caused by the high acceptor doping in the CuI ($N_A=10^{20}$ cm⁻³). For such a thin potential barrier most of the electrons can tunnel through at or near the base of the barrier and so the current across the interface is not blocked at all. We conclude that the spike is not limiting the efficiency of the cell.

4. Conclusions

We have added a model for intra-band tunneling to SCAPS. This allows to correctly simulate the current transport properties of a heterointerface, within the limitations of the WKB approximation. In comparison with earlier attempts to incorporate intra-band tunneling in a numerical device simulator, we use an improved model in which the tunnel current is injected at the correct position within the cell.

For the CISCuT solar cell with a CuI buffer layer, we conclude that the spike at the CuI/CuInS₂ interface poses no limitations on the light current over the interface, and is thus not limiting the solar cell efficiency.

Acknowledgement

This work was supported in part by the Research Fund of the University of Gent (BOF-GOA).

References

- [1] M. Burgelman, J. Verschraegen, S. Degraeve, P. Nollet, Prog. Photovolt. 12 (2004) 143.
- [2] M. Burgelman, P. Nollet, S. Degraeve, Thin Solid Films 361–362 (2000) 527.
- [3] J. Penndorf, M. Winkler, O. Tober, D. Roser, K. Jakobs, Sol. Energy Mater. Sol. Cells 53 (1998) 285.
- [4] M. Winkler, J. Griesche, I. Konovalov, J. Penndorf, J. wienke, O. Tober, Sol. Energy 77 (2004) 705.
- [5] C.B. Duke, Tunneling in Solids, Academic Press, New York, 1969.
- [6] K.H. Gundlach, J.G. Simmons, Thin Solid Films 4 (1969) 61.
- [7] S.J. Fonash, Solar Cell Device Physics, Academic Press, New-York, 1977.
- [8] K. Yang, J.R. East, G.I. Haddad, Solid-State Electron. 36 (1993) 321.
- [9] R. Stratton, Phys. Rev. 125 (1962) 67.
- [10] J. Verschraegen, M. Burgelman, J. Penndorf, Proc. 20th European Photovoltaic Solar Energy Conference (Barcelona, E, June 2005), WIP, München, 2005, p. 1835.